Can magnetotail reconnection produce the auroral intensities observed in the conjugate ionosphere?

N. Østgaard,[1] K. Snekvik,[1] A. L. Borg,[2] A. Åsnes,[3] A. Pedersen,[4] M. Øieroset,[5] T. Phan,[5] and S. E. Haaland[1,6]

Received 20 February 2009; revised 20 February 2009; accepted 20 March 2009; published 3 June 2009.

[1] In a recent case study, Borg et al. (2007) reported that an inverted V structure, caused by a field-aligned potential drop of 30 kV producing very strong X-ray aurora, was found in connection with tail reconnection. However, the in situ particle measurements indicated clearly that the particles responsible for the X-ray aurora were not accelerated by the reconnection process. In this article, we report the predicted auroral intensities of thirteen reconnection events where Cluster passed through the reconnection region. For six of the events, global auroral imaging data were available and the predicted auroral intensities could be compared with the observed intensities. Our main findings are as follows: (1) Acceleration in the reconnection region is generally not sufficient to account for the observed auroral intensities. (2) Additional acceleration between the reconnection region and the ionosphere is needed to explain the auroral intensities. Although we see signatures that point toward potential drops at the flanks of bursty bulk flows (BBFs), we also find signatures of Alfvén wave accelerated electrons at 700 km and we are not able to determine the most likely acceleration mechanism. (3) The reconnection events are observed 2–14 min after substorm onset and indicate that reconnection is an expanding process observed along the poleward boundary of the aurora.

Citation: Østgaard, N., K. Snekvik, A. L. Borg, A. Åsnes, A. Pedersen, M. Øieroset, T. Phan, and S. E. Haaland (2009), Can magnetotail reconnection produce the auroral intensities observed in the conjugate ionosphere?, *J. Geophys. Res.*, *114*, A06204, doi:10.1029/2009JA014185.

1. Introduction

[2] Magnetic reconnection is a fundamental plasma process by which magnetic energy is converted to kinetic energy. Reconnection is also an important process to explain how solar wind energy can be transferred through the Earth's magnetic shield. According to the anti-parallel paradigm [*Crooker*, 1986] reconnection is most efficient when the interplanetary field has a strong southward component that is anti-parallel to the Earth's magnetic field at the dayside magnetopause. Magnetic reconnection leads to opening of magnetic flux on the Earth's dayside and a direct entrance of solar wind particles into the magnetosphere. Because of the frozen-in condition in the collisionless solar wind plasma the newly opened magnetic flux tubes will be draped down the tail of the magnetosphere, where magnetic reconnection is again required to balance the amount of magnetic flux in the magnetosphere. This constitutes a continuous opening-closing magnetic flux cycle [*Dungey*, 1961]. Depending on the reconnection rate on the dayside the magnetotail reconnection can either occur several hundreds of R_E's down the tail to create the far X line or, when the dayside reconnection rate is high, between 15–25 R_E in order to maintain total pressure balance in the system [*Lockwood*, 1997]. This latter location is the Near-Earth Neutral Line (NENL) and is thought to have important implications for substorm triggering and production of intense global auroral emissions [*Baker et al.*, 1996]. As reported by *Nagai* [2006] the NENL also moves closer to the Earth as the solar wind energy input increases.

[3] There are several ways to observe ionospheric effects of magnetotail reconnection or to deduce information about the reconnection process by examining the ionospheric signatures. As the poleward boundary location of the auroral oval can be used as a proxy for the amount of open magnetic flux in the polar cap, the expansion (opening on the dayside) and contraction (closing on the nightside) of the auroral oval is indeed an ionospheric signature of the Dungey cycle and can be used to estimate quantitatively the dayside and nightside reconnection rates [*Hubert et al.*, 2006; *Milan et al.*, 2007]. Reconnection rate can also be estimated from the ion flow across the open-closed boundary, an approach based on integrating the Faraday's law along a closed loop defined by the separatrix [*Vasyliunas*, 1984] and has been reported in several articles [*de la*

[1]Department of Physics and Technology, University of Bergen, Bergen, Norway.
[2]Norwegian Defence Research Establishment, Kjeller, Norway.
[3]SRE-OSC, Energy Systems Technology and Education Center, Noordwijk, Netherlands.
[4]Department of Physics, University of Oslo, Oslo, Norway.
[5]Space Sciences Laboratory, University of California, Berkeley, California, USA.
[6]Solar Physics Research, Max-Planck Institute, Lindau, Germany.

0148-0227/09/2009JA014185

Beaujardiére et al., 1991; *Blanchard et al.*, 1996; *Ober et al.*, 2001; *Østgaard et al.*, 2005]. As magnetic reconnection is an energy transformation process, where magnetic energy is transformed to kinetic energy of the plasma, the NENL reconnection process can be observed remotely by detecting fast flows or bursty bulk flows (BBFs) in the plasma sheet [*Baumjohann et al.*, 1990; *Angelopoulos et al.*, 1992]. Fast flows and BBFs lead to flow shears and field-aligned currents at their flanks. If the conductivity along the field lines is low [*Shiokawa et al.*, 2000] parallel electric fields are required to preserve current continuity. Particles from the magnetosphere will then be accelerated along the magnetic field lines and can be observed by low altitude satellites as enhanced electron fluxes at the energies corresponding to the potential drop [*Evans*, 1974]. Remote signatures of BBFs have been observed both as enhanced plasma flows in the ionosphere [*de la Beaujardiére et al.*, 1991] and by global auroral imaging [*Nakamura et al.*, 2001]. Magnetic reconnection may also occur in a pulsed manner and such magnetic perturbations can give rise to Alfvén waves that can accelerate particles [*Wygant et al.*, 2000] and be observable in the ionosphere [e.g., *Chaston et al.*, 2007]. Alfvén waves are most commonly found at the open-closed boundary in the premidnight sector and this is also where the wave power is largest [*Chaston et al.*, 2003]. As the particle distributions in the ionosphere resulting from this process will have a power law distribution with average energies typically below 1 keV, often called super-thermal electrons, they are distinguishable from the electrons accelerated by a potential drop with typical average energies of several keVs. The polar boundary intensification (PBI) and tail flow bursts reported by *Lyons et al.* [2002] were found to be manifestations of ultralow frequency (ULF) waves in the solar wind. The PBIs might be associated with such Alfvén accelerated electron distributions as both PBIs and Alfvén waves are most commonly observed at the open-closed boundary in the midnight sector. However, *Lyons et al.* [2002] also found a close connection between PBIs and BBFs, which would indicate that the observed aurora is produced by electrons accelerated by a potential drop. Auroral signatures associated with flow shears and BBFs (potential drop) and PBIs (Alfvén waves or potential drop) might therefore be indirect signatures of magnetic reconnection. One could also argue that the acceleration of the electrons in the reconnection region [*Pritchett*, 2006; *Åsnes et al.*, 2008] and/or the Hall current along the magnetic field lines out of the reconnection region [*Fujimoto et al.*, 2001; *Snekvik et al.*, 2008] can be observable in the ionosphere [*Treumann et al.*, 2006]. While some argue that acceleration in the reconnection region can be significant [*Øieroset et al.*, 2002; *Pritchett*, 2006] others claim that the energy gain from magnetic annihilation in the magnetotail is very small [*Yoon and Lui*, 2006].

[4] The purpose of the present study is to examine if the reconnection process can produce observable intensities of auroral UV and X-ray emissions in the conjugate ionosphere or whether auroral emissions result from processes that are just indirectly related to magnetic reconnection [*Imada et al.*, 2007]. Such indirect connections could be the flow shears of BBFs or Alfvén wave accelerated electrons. This study is motivated by a recent case study [*Borg et al.*, 2007] based on data from Cluster, Polar Ionospheric X-ray Imaging Experiment (PIXIE) [*Imhof et al.*, 1995] and SSJ/4 electrostatic analyzer [*Hardy et al.*, 1984] on Defence Meteorological Satellite Program (DMSP). In that article we reported that a very strong X-ray aurora was found at the Cluster foot point just at the time Cluster passed through the reconnection region. At a first glance we thought the X-ray spot was directly connected to acceleration in the reconnection region. However, the in situ particle measurements by Cluster indicated clearly that the particles responsible for the X-ray aurora were not accelerated by the reconnection process. The very intense inverted V structure caused by a field-aligned potential drop of 30 kV points to flow shears at the flanks of a BBF as the acceleration mechanism. The current study has a similar approach, but now we analyze twelve more events to investigate whether magnetotail reconnection can produce the auroral intensities observed at the ionospheric foot point of the reconnection event.

[5] Our approach is the following.

[6] 1. Cluster magnetic and plasma data are used to identify the reconnection region.

[7] 2. The 1-min averaged electron data from Cluster covering electrons from 30 eV to 450 keV are used to estimate the predicted ultraviolet emissions and X rays in the ionosphere that would be seen by auroral global imagers. Only data obtained when the spacecraft are in the outflow region are used for these estimates.

[8] 3. For six of the events where we have global imaging data of ultraviolet (UV) emissions or X-ray emissions we have mapped the Cluster position to the ionosphere using three different Tsyganenko models, T89, T96 and T01 [*Tsyganenko*, 1989, 1995, 2002].

[9] 4. Then we compare and discuss the predicted intensities versus the observed intensities relative to the time of the earthward flows. These events are also discussed in the context of global substorm activity and the expansion of the open-closed boundary.

2. Observation

[10] The Cluster data reported here are sampled from August to October in 2001, 2002, 2003 and 2004. This is the time of the year the Cluster spacecraft spent time in the plasma sheet at 15 to 19 R_E and were in a good position to make in situ observations of the reconnection region. The separation of the spacecraft varied from about 200 km in 2003 to about 4000 km in 2002. We are also using data from Imager for Magnetopause-to-Aurora Global Exploration (IMAGE), DMSP, Polar satellites. The data format and instrument details needed for understanding will be explained as we present our observations. To describe the analysis we will first present three of the events where we had both Cluster, IMAGE (or Polar) and low-altitude satellite data. Then we present three more events with Cluster and IMAGE data and finally seven events where only Cluster data were available.

2.1. Three Events With all Data Available

[11] To identify the reconnection region we have used data from the Cluster Ion Spectrometry experiment (CIS) [*Reme et al.*, 2001] and the Cluster magnetic field experiment (FGM) [*Balogh et al.*, 2001]. CIS has two sensors, CODIF and HIA, and the calibrated data have time reso-

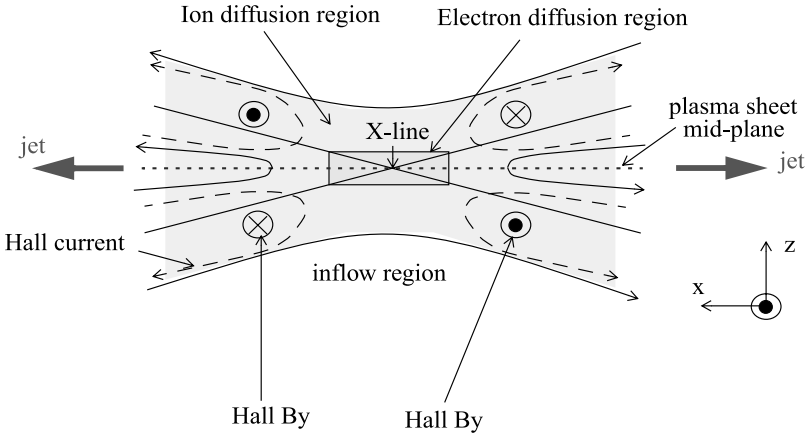

Figure 1. Two-dimensional magnetic reconnection as adapted from *Sonnerup* [1979].

lutions of 8 sec and 12 sec, respectively. We are using HIA data from Cluster 3 and CODIF data from Cluster 1 and 4. The time resolution of the FGM data is 0.2 sec (5 Hz). Data from the years 2001–2004 between 1 August and 15 November were examined to find magnetic reconnection events in the magnetotail [*Borg*, 2006]. Two assumptions have been made for this procedure. First, we assume that the reconnection region could be represented as a two-dimensional structure in the *XZ* plasma sheet plane, as shown in Figure 1. Second, the reconnection region is assumed to move over the spacecraft in approximately the *X* direction. The Cluster data are transformed into a coordinate system based on the orientation of the current sheet. At the distances studied here, the neutral sheet is oriented on average approximately parallel with the XY_{GSM} plane [*Kaymaz et al.*, 1994]. As our time intervals include both positive and negative B_Z a minimum variance analysis to find the plasma sheet normal cannot be applied. Our best choice is therefore to let $\mathbf{Z} = \mathbf{Z}_{GSM}$ well aware that this is as an average plasma sheet normal. Close to midnight the main component of the magnetic field is approximately along X_{GSM}, but as the distance from midnight increases, the component along Y_{GSM} increases because of the flaring of the magnetotail [*Kaymaz et al.*, 1994]. To account for this, a variance analysis of the magnetic field data is performed. We have used a time window similar to the event interval. The direction with maximum variance **l**, is taken as the *X* direction. This can be done for current sheets where the current is approximately unidirectional [*Khrabrov and Sonnerup*, 1998]. The modified *Y* direction is parallel with $\mathbf{Z}_{GSM} \times \mathbf{l}$. All the Cluster data shown in Figures 2–7 are rotated into this coordinate system.

[12] In Figure 2a the magnetic perturbations (B_y) as a function of V_x and B_x are shown for the time interval 0502 UT to 0510 UT on 15 September 2001 observed by Spacecraft 1 (SC1), 3 (SC3) and 4 (SC4) when Cluster were located at [−16.6, 7.8, −2.6] R_E GSM. Black circles indicate negative B_y into the plane and red circles are positive B_y out of the plane. The data used to create this plot are shown in Figure 2b, 2C and 2D, where SC1 is black, SC3 is green and SC4 is blue. As the sign and magnitude of B_x can be used as a proxy for where Cluster is relative to the center of the plasma sheet and the V_x gives information whether the spacecraft is located earthward or tailward of the X line, the observed B_y perturbations can be directly compared to expected magnetic perturbations from the Hall current system predicted by [*Sonnerup*, 1979] and shown in Figure 1. The B_y perturbations are indeed organized as the expected quadrupolar Hall magnetic signatures and we consider this as a strong indication of Cluster being inside or at least close to the reconnection region. In addition, the sign of B_z (Figure 2e) is changing consistent with this picture, with positive B_z during earthward flow and negative B_z during tailward flow. The earthward flow is fast and reaches 1120 km/s at 0507 UT.

[13] It should be noted that quadrupolar signatures have been observed at some distance from the reconnection region [e.g., *Fujimoto et al.*, 2001; *Ueno et al.*, 2003] and that the frozen-in condition has been found to be fairly satisfied even when quadrupolar signatures, B_z and flow reversals have been observed [*Runov et al.*, 2008; *Sergeev et al.*, 2008]. As we have not performed the necessary analysis of the electric field and plasma measurements, we cannot determine the precise time intervals when the spacecraft resided in the ion diffusion region where the frozen-in condition breaks down. However, by seeing at least three (and in many cases four) of the quadrupolar signatures along with the reversals we do believe we are close enough to claim that the observed electron distributions have not been accelerated by other processes than reconnection. Throughout the text we therefore refer to the reconnection region rather than the ion diffusion region.

[14] For all the events identified in this study the three criteria for identifying the reconnection region are used; (1) a flow reversal in the *X* direction, (2) a simultaneous B_z reversal and (3) a quadrupolar (or at least 3 of them) Hall magnetic B_y perturbation in a $V_x - B_x$ frame.

[15] To investigate whether the acceleration in the reconnection region can be responsible for any observable auroral intensities we have used 1-min averages of the electron data from the Plasma Electron And Current Experiment (PEACE) [*Johnstone et al.*, 1997] and the Research with Adaptive Particle Imaging Detectors (RAPID) [*Wilken et al.*, 2001] from SC 1. To make sure that only data from the outflow region are included in the 1-min average spectra we only sample data when $V_x \geq 0.5 \times \max(V_x)$, where $\max(V_x)$ is the maximum within the time interval we analyze. For some of the events, this criterion leads to some data gaps. From the

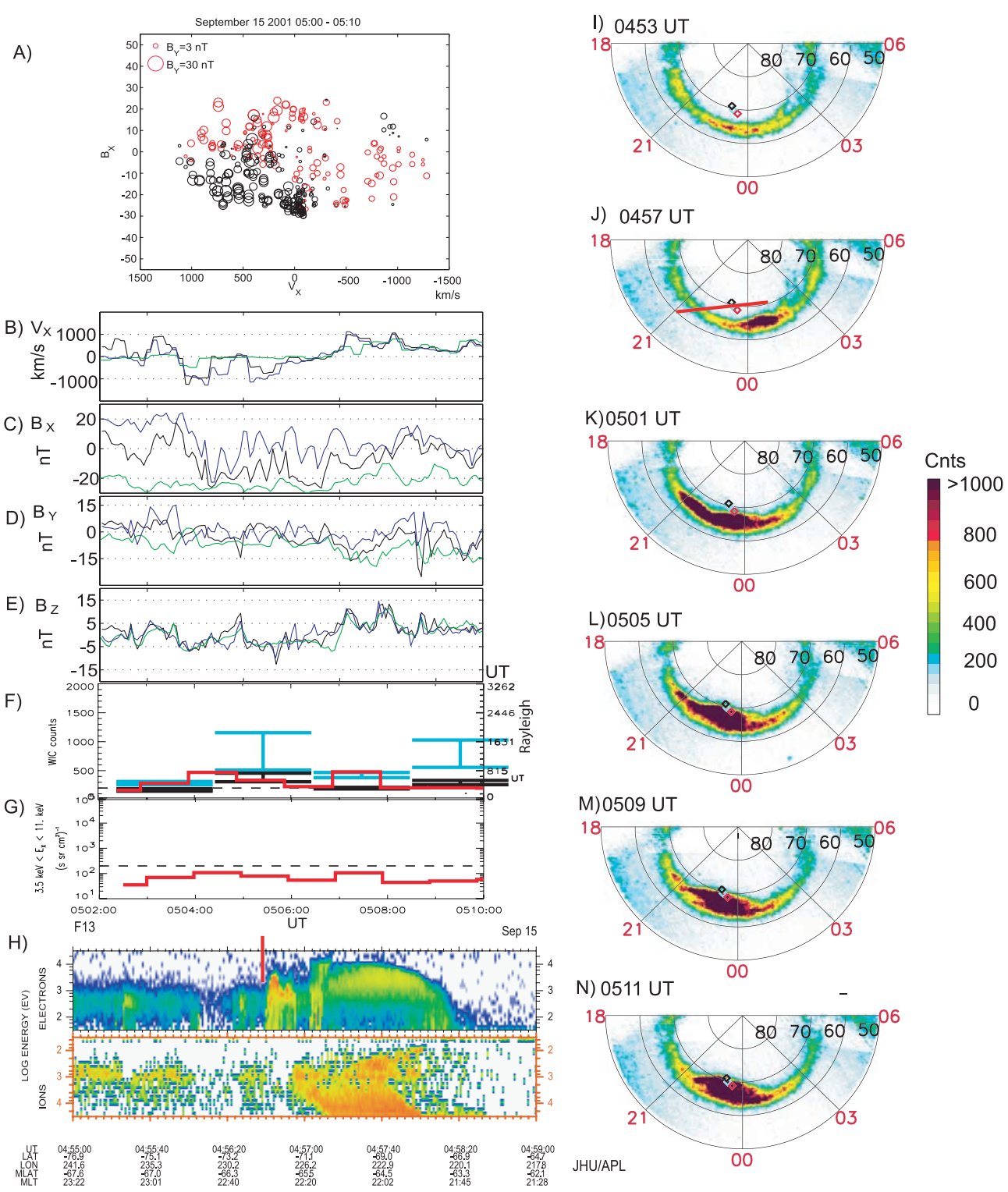

Figure 2. (a–e) Measurements by Cluster SC1 (black), SC3 (green), and SC4 (blue) for 15 September 2001, 0502–0510 UT rotated into a coordinate system based on the orientation of the plasma sheet plane. (Figure 2a) B_y perturbations (black is negative and red is positive) as a function of V_x and B_x, (Figure 2b) V_x, (Figure 2c) B_x, (Figure 2d) B_y, (Figure 2e) B_z, (f) UV emissions; predicted in red, observed at the T89 foot point in cyan, observed at T01 foot point in black. The dashed line is the noise level of WIC after background subtraction. (g) Predicted X rays, 3.5–11 keV, as for the PIXIE camera. Dashed line is the noise level for PIXIE. (h) DMSP F13 measurement passing through the oval as shown in Figure 2j. (i–n) WIC images with T89, T96, and T01 foot point indicated as cyan, red, and black diamonds.

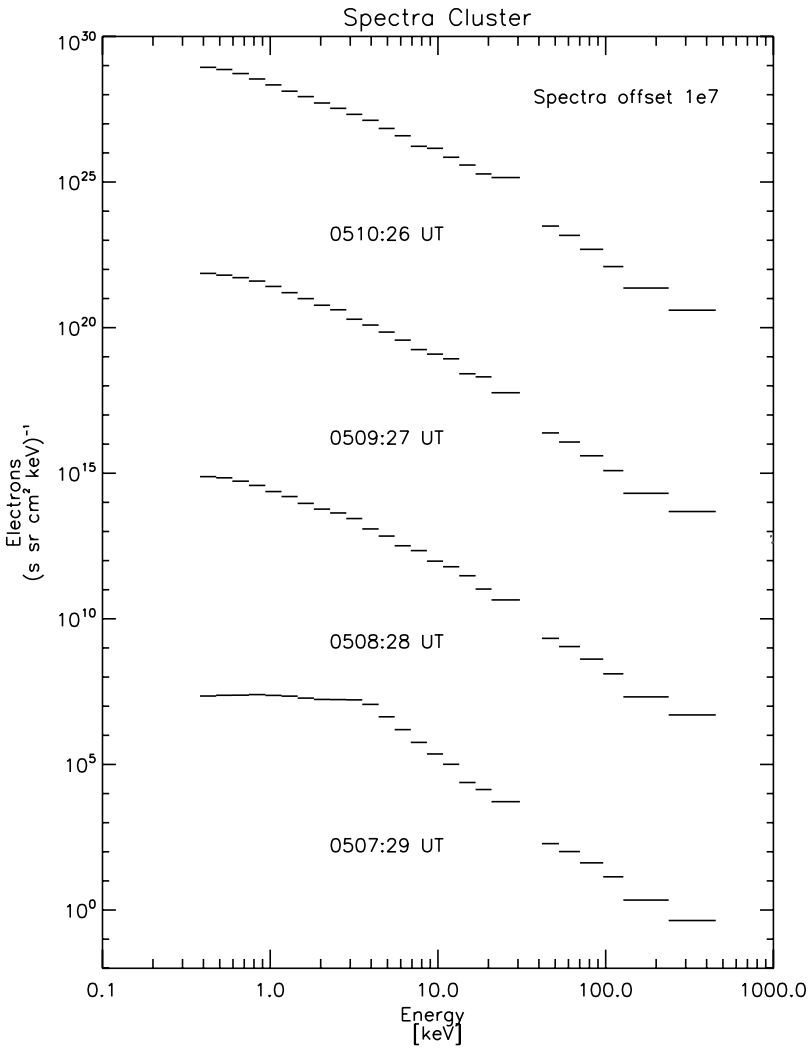

Figure 3. Four 1-min averaged composite PEACE and RAPID spectra (SC1) from 0507 UT to 0511 UT when strong Earthward flows were observed by Cluster.

PEACE experiment differential electron fluxes in 23 channels from 156 eV to 26.7 keV are obtained within ±7.5° pitch angle. From the RAPID instrument only spin averaged data are available in 6 energy channels from 41.7 keV to 453 keV. We have combined these two data sets to estimate the predicted UV signatures from electrons in the energy range from 156 eV to 453 keV, as shown in Figure 3 well aware that the electrons above 20 keV do not contribute much to the estimated emissions that would be observed by an auroral imager like the Far Ultraviolet (FUV) Wide band Imaging Camera (WIC) [*Mende et al.*, 2000] on IMAGE. This means that most of the UV emissions we estimate results from the electrons observed by PEACE. Given the pitch angle resolution of the PEACE instrument we have to assume that the fluxes within ±7.5° pitch angle are representable for the electron distribution in the much smaller loss cone (∼1°) at Cluster location.

[16] To estimate the predicted count rates for IMAGE WIC we have convolved the PEACE spectra with the WIC response function [*Frey et al.*, 2003]. The estimates are shown by a red histogram in Figure 2f with the dashed line indicating the noise level in WIC after background subtraction. The noise level is determined from pixels outside the auroral region and is found to be about 200 cnts/pixel. Only during the time intervals 0504–0506 UT and 0507–0508 UT do the fluxes of electrons measured by Cluster predict UV emissions slightly above the noise level. The total electron energy flux above 100 eV never exceeds 1.4 mW/m^2.

[17] In Figure 2g we show the predicted X-ray counts in the energy range 3.5–11 keV, similar to PIXIE camera onboard Polar satellite. Although these X rays are produced by all electrons above 3.5 keV, the X-ray production is nonlinearly increasing with electron energy. This means that electrons measured by both PEACE and RAPID will contribute to the X-ray flux. These estimates are therefore good indicators for determining the effects of energetic electrons from the reconnection region. For the entire interval, the predicted X-ray fluxes are below the noise level of PIXIE, shown by the dashed line. For more details on how we estimate the X-ray fluxes we refer to *Østgaard et al.* [2000, 2001] and *Borg et al.* [2007].

[18] One-minute average spectra from SC3 and SC4 (not shown) give similar predictions and the total electron energy fluxes never exceed 0.7 mW/m^2 and 1.7 mW/m^2, respectively.

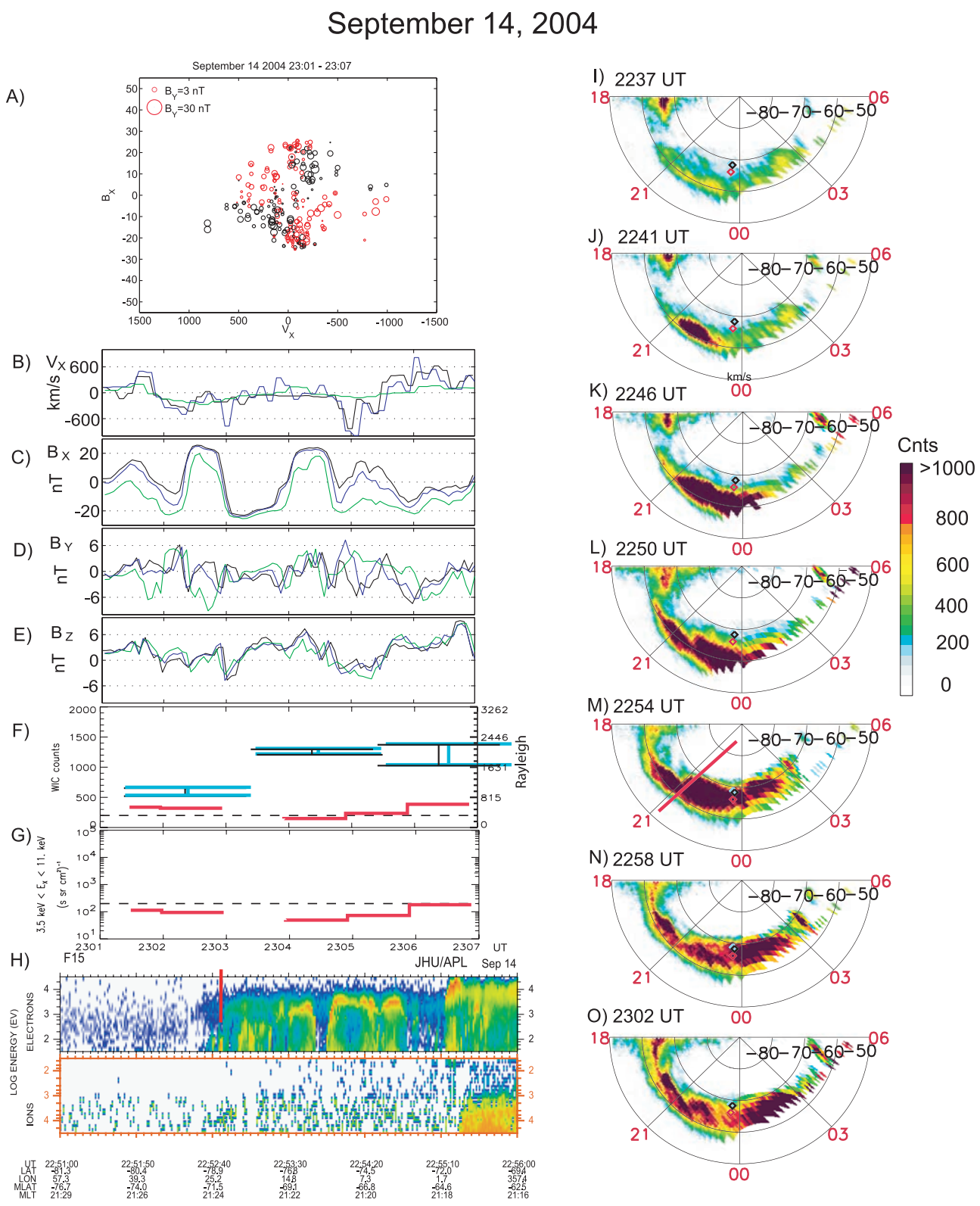

Figure 4. Same as in Figure 2 but for 14 September 2004, except that we now have DMSP 15 in Figure 2h and its track is shown in Figure 2m.

[19] In Figures 2i–2n the WIC images are displayed with the foot point of Cluster using three different Tsyganenko models, T89, T96 and T01 as shown with cyan, red and black diamonds, respectively. These foot points are highly uncertain when NENL is forming, but this is the best we can do. In this case the three Tsyganenko models predict fairly similar foot points. However, as will be seen, T89 and T01 foot points usually converge, while T96 gives a different

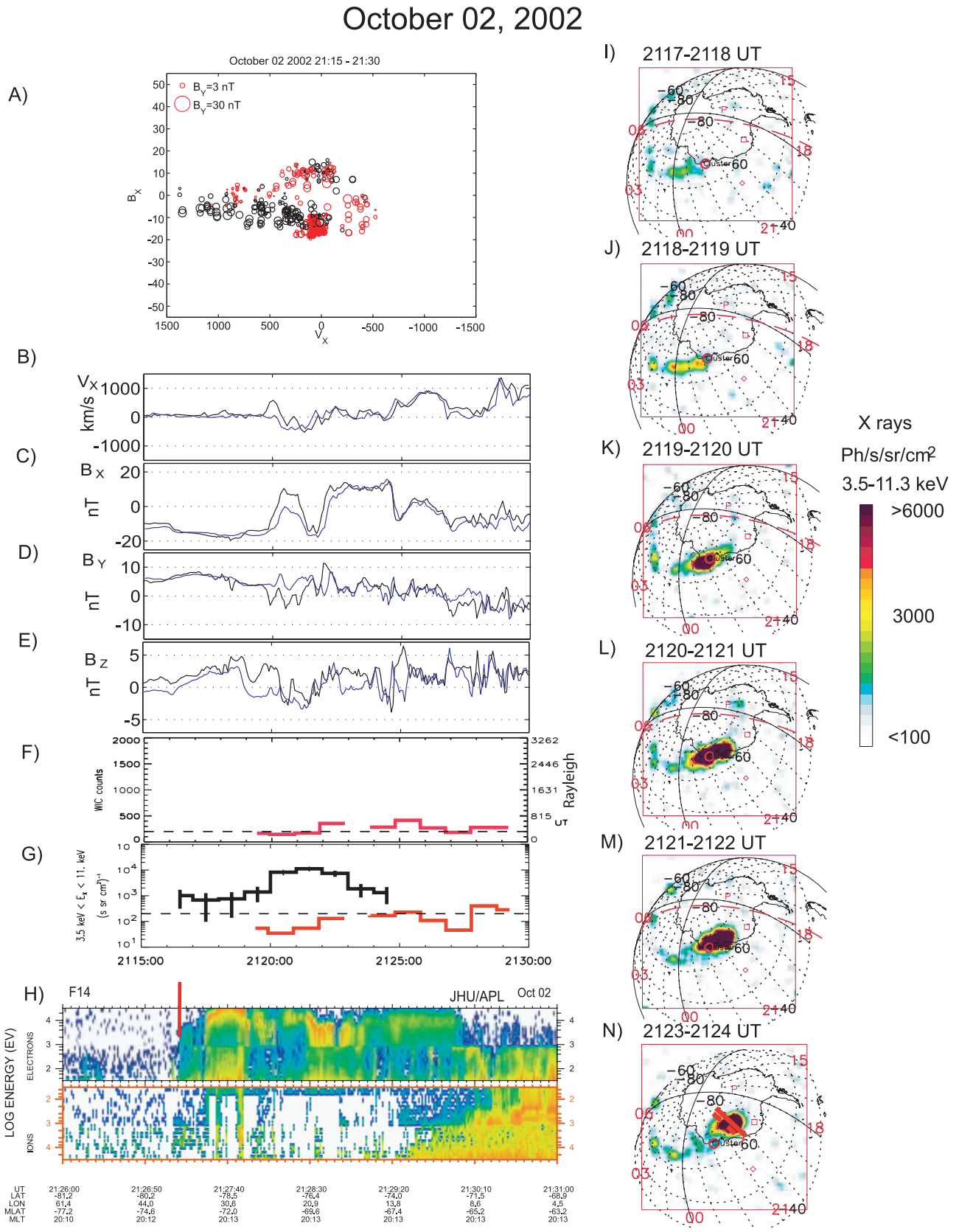

Figure 5. Similar as in Figure 2 but for 2 October 2002, except that we show X-ray images from PIXIE in Figures 2h to 2m, expected and observed fluxes in Figure 2f are for X rays, DMSP 14 in Figure 2g and its track is shown in Figure 2m. This figure is a composite of figures from *Borg et al.* [2007].

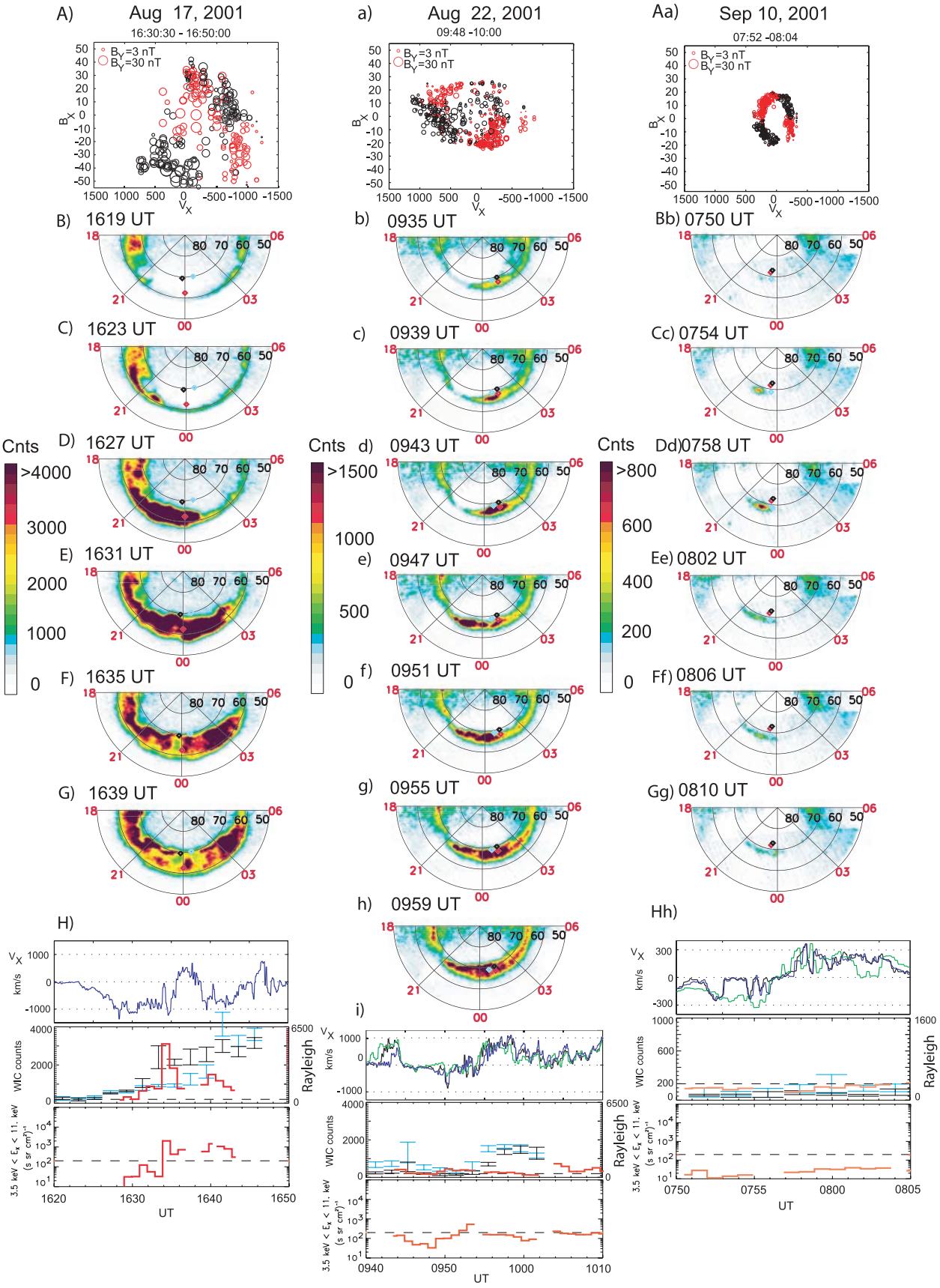
A) Aug 17, 2001
16:30:30 - 16:50:00
a) Aug 22, 2001
09:48 -10:00
Aa) Sep 10, 2001
07:52 -08:04
B) 1619 UT
b) 0935 UT
Bb) 0750 UT
C) 1623 UT
c) 0939 UT
Cc) 0754 UT
D) 1627 UT
d) 0943 UT
Dd) 0758 UT
E) 1631 UT
e) 0947 UT
Ee) 0802 UT
F) 1635 UT
f) 0951 UT
Ff) 0806 UT
G) 1639 UT
g) 0955 UT
Gg) 0810 UT
h) 0959 UT
H)
Hh)
i)
Cnts
WIC counts
Rayleigh
UT

Figure 6

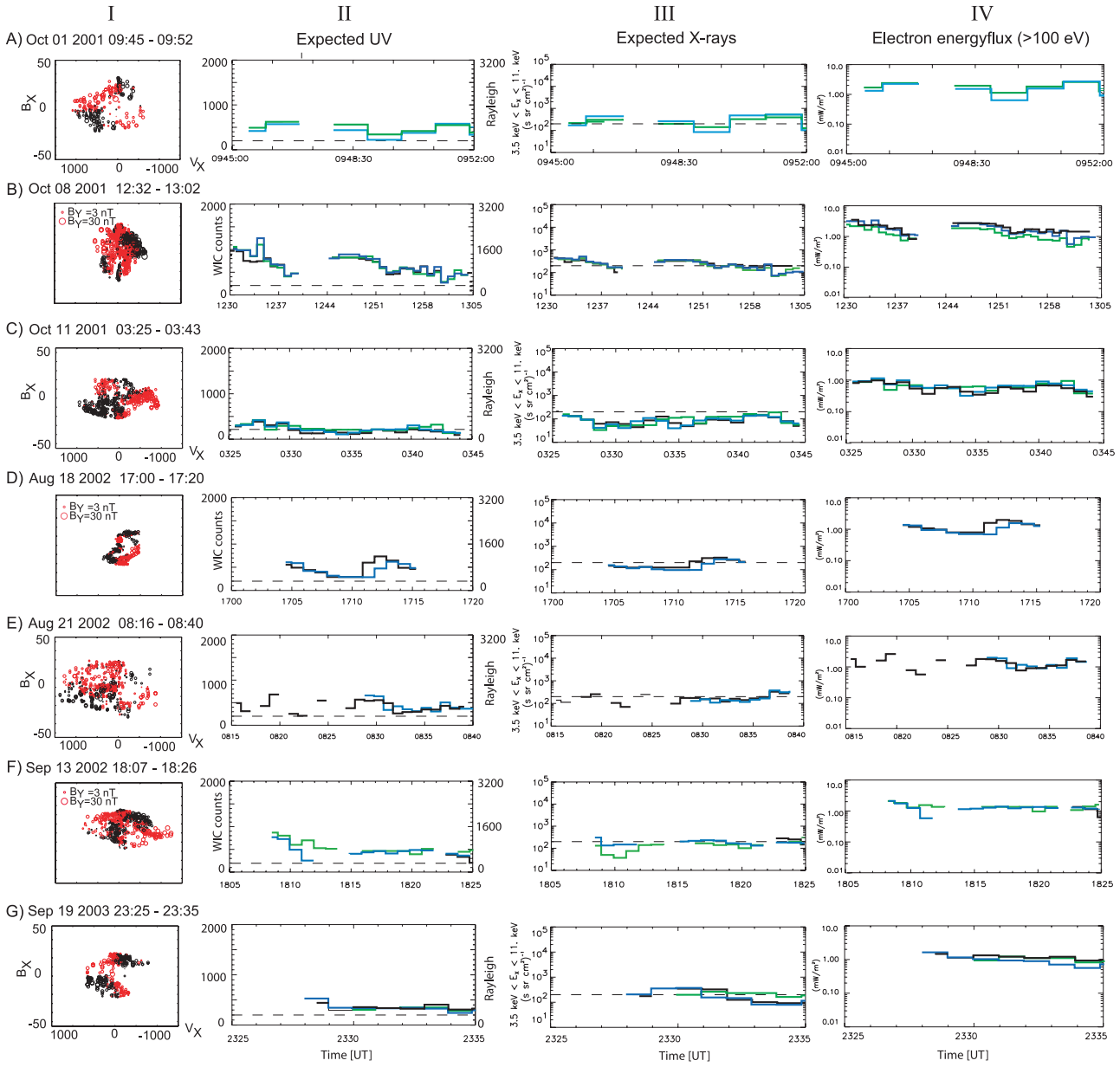

Figure 7. (a–g) Seven encounters of the reconnection region by Cluster. The columns show the following: (I) B_y perturbations as a function of V_x and B_x using data from SC1, SC3 and SC4, except (Figure 7e) 21 August 2001 where only SC1 and SC3 are used. (II) Predicted UV emissions based on PEACE and RAPID data. Red circles mark predictions when earthward flows are observed. (III) Predicted X rays (3.5–11 keV) based on PEACE and RAPID electron spectra. (IV) Total electron energy flux (≥100 eV). In columns II, III and IV, black is used for SC1; green, for SC3; and blue, for SC4.

foot point. In Figure 2f the intensities observed by WIC at the T89 and T01 estimated Cluster foot points are shown with cyan and black. The error bars are maximum and minimum WIC counts in a ±1.5° longitudinal and ±0.5° latitudinal area around the foot point. We want to point out the following.

[20] 1. A substorm break-up is observed just before 0457 UT (Figure 2j)

Figure 6. Cluster and IMAGE data for 17 August 2001, 22 August 2001, and 10 September 2001. (A, a, and Aa) B_y perturbations as a function of V_x and B_x using data from SC 4 for 17 August 2001 and from SC1, SC2, and SC4 for 22 August and 10 September 2001. (B–G, b–h, and Bb–Gg) WIC images with T89, T96, and T01 foot point indicated as cyan, red, and black diamonds. (H, h, and Hh) Cluster V_x (SC4 and SC1 + SC2 + SC4), UV emissions, predicted from SC1 spectra (except in Figure 6H where SC4 is used) in red observed at the T89 foot point in cyan, observed at T01 foot point in black. The dashed line is the noise level of WIC after background subtraction. Figure 6Hh shows the predicted X rays, 3.5–11 keV (red), from SC1 spectra.

[21] 2. Eight to 10 min later (0505 UT or 0507 UT), the expansion of the substorm bulge reaches Cluster foot point. The foot point estimated by T96 indicates that the bulge reaches Cluster earlier, at 0501 UT.

[22] 3. Cluster sees a flow reversal with a subsequent fast earthward flow speed of 1120 km/s at 0506–0507 UT. Fast earthward flow is also seen at 0502 UT.

[23] 4. The predicted UV emissions from Cluster electron measurements are weaker (maximum 500 cnts) than what are observed at the poleward edge of the bulge (500–1000 cnts or 0.8–1.6 kR).

[24] 5. There are no predicted X-ray fluxes.

[25] Finally we show the best available low altitude satellite pass during this interval in Figure 2h. DMSP F13 entered the oval from the polar cap in the opposite hemisphere just before 0457 UT (trajectory is shown by red line in Figure 2j). Although this is at the very westward edge of the break-up, relatively intense electron precipitation peaking at a few keV due to a potential drop is clearly seen at 0456.40 UT when DMSP crossed the open-closed boundary, marked with a red vertical line in Figure 2H. We cannot make any strong statement from this, but accelerated electrons by a potential drop points to acceleration mechanism associated with flow shears at the flanks of a BBF giving divergent electric fields and potential drop along the field to maintain current continuity. At the Cluster foot point location, however, we can only say that electrons from the reconnection region cannot produce the observed auroral intensities.

[26] Similar plots are shown in Figures 4a–4o for the reconnection event encountered by Cluster on 14 September 2004, 2301 UT–2307 UT. Cluster were at [−18.1, 2.1, −0.7] R_E GSM. Figure 4a, using SC1, SC3 and SC4, shows a clear quadrupolar signature of B_y as a function of V_x and B_x. The best available low altitude satellite observations were from DMSP F15 in the southern hemisphere entering the substorm bulge (trajectory shown in red in Figure 2m) from the polar cap at 2252:40 UT marked with red vertical line in Figure 2h. In this case T96 model estimates Cluster foot point (red diamond) a few degrees equatorward of what T89 and T01 estimate (cyan and black diamonds, respectively). We want to point out the following.

[27] 1. Substorm break-up was observed just prior to 2241 UT (Figure 2j).

[28] 2. The bulge reached the Cluster foot point, as estimated by T89 and T01, at 2254 UT 13 min after the break-up (Figure 2m).

[29] 3. Three intervals of earthward flows are seen with maxima at 2301:30 UT, 2304 UT and 2306 UT reaching ~600–800 km/s (Figure 2b).

[30] 4. The predicted UV emissions from the electron measurements (SC1) are just above the sensitivity level of WIC while the observed emissions at foot point T89 and T01 are 500–1500 cnts (0.8–2.5 kR). The maximum total electron energy flux is 1.3 mW/m^2.

[31] 5. There are no predicted X-ray emissions.

[32] 6. SC3 and SC4 give similar predictions (not shown) with maxima of 1.8 mW/m^2 and 1.3 mW/m^2, respectively.

[33] 7. DMSP F15 measures enhanced fluxes of low energy electrons when passing the open-closed boundary at 2252:40 UT as marked with a red vertical line indicating that the electrons have been weakly accelerated by Alfvén waves. Again, we see indication at DMSP location westward and earlier than Cluster of electrons being accelerated not in the reconnection region, but along the field lines between the reconnection region and the ionosphere. However, at Cluster foot point we can only conclude that there must be additional acceleration to reconnection.

[34] For completeness we have included the event on 2 October 2002, that was reported by *Borg et al.* [2007] in the same format as Figures 2 and 4 but now with X-ray images instead of UV images (Figure 5). Cluster SC1 (black) and SC4 (blue) are used in Figures 5a–5e. As only measurements from the outflow region are included when calculating 1-min average spectra, the predicted X-ray fluxes deviate slightly from what were shown by *Borg et al.* [2007]. We want to point out the following.

[35] 1. A very strong auroral X-ray intensification was observed at 2119 UT (Figures 5j and 5k).

[36] 2. The Cluster foot point, as estimated by T89, was inside the region with intensified X-ray aurora.

[37] 3. Earthward flows were seen with maximum at 2120 UT and 2125 UT reaching 1380 km/s at 2129 UT (Figure 5b).

[38] 4. The predicted UV emissions from the electron measurements from SC1 are just above the sensitivity level of WIC (~300 R). Although the UV emissions seen by UVI on Polar (not shown here, but see *Borg et al.* [2007]) were weak (1.5–2 kR) they were well above the predicted UV intensities. The maximum of total electron energy flux is only 1.2 mW/m^2.

[39] 5. There are no predicted X-ray emissions, but an unusual intense X-ray auroral spot is seen.

[40] 6. SC3 and SC4 give similar predictions (not shown) with maximum energy flux of 0.9 mW/m^2 and 1.0 mW/m^2, respectively.

[41] 7. When entering closed field lines at 2127:10 UT (marked with red vertical line) DMSP F14 sees plasma sheet electrons of a few keV. However, 20 seconds later, at 2127:30 UT, the spacecraft passes through a very large inverted V signature of ~30 kV. As discussed by *Borg et al.* [2007] the DMSP spectra are consistent with both the UV emissions and the X-ray emissions. Electrons accelerated by a potential drop are consistent with flow shears at the flanks of the high-speed earthward flows.

2.2. Three More Events With Imaging Data

[42] Now we will show three more events where we have Cluster and global imaging data but no low altitude satellite data close enough in time to know the electron distribution impacting the ionosphere at the open-closed boundary. Data from 17 August 2001, 20 August 2001 and 10 September 2001 are shown in Figure 6. Notice that we have used different color scale for the two events, because 17 August is an intense auroral event while 10 September is a very weak event. Going from the top for the three events we want to emphasize.

[43] 1. Both 17 and 22 August are high-speed flow events with earthward flow speeds of 800–1120 km/s, while for 10 September, the maximum flow speed is low (365 km/s).

[44] 2. On 17 August, the substorm breakup occurs at 1623 UT and the bulge reaches Cluster at 1633 UT (10 min later). On 22 August, the substorm starts at 0939 UT and the bulge reaches Cluster foot point at 0953 UT (14 min later) and

Table 1. Maximum Electron Energy Flux[a]

Date	SC1 (mW/m^2)	SC3 (mW/m^2)	SC4 (mW/m^2)
15 September 2001	1.4	0.7	1.7
14 September 2004	1.3	1.8	1.3
2 October 2001	1.1	0.9	1.0
17 August 2001	8.0	–	11.0
22 August 2001	2.0	–	1.6
10 September 2001	0.4	0.4	0.4
1 October 2001	–	2.1	2.7
8 October 2001	2.7	2.1	2.7
11 October 2001	1.0	0.9	1.1
18 August 2002	2.0	–	1.7
21 August 2002	2.6	–	1.9
13 September 2002	1.4	2.2	2.2
19 September 2003	1.5	1.3	1.9

[a]Energy flux $\geq$100 eV is calculated from 1-min average spectra of PEACE and RAPID data in the outflow region.

on 10 September, the small intensification starts at 0754 UT and gets close to Cluster foot point 4 min later at 0758 UT.

[45] 3. As seen in Figures 6i and 6Hh (where spectra from SC1 are used), there are no prediction of X-ray aurora. However, for 17 August 2001, Figure 6H, where we have shown SC4 spectra due to the better coverage, we do predict X-ray emissions that might have been observable. Even more interesting is that the PEACE/RAPID spectra predict UV emissions in the same range as observed at 1634–1636 UT. However, at the end of the interval the predicted emissions are significantly lower than observed emissions. The maximum total electron energy flux measured by SC1 and SC4 is also significantly higher and reaches 8 mW/m^2 and 11 mW/m^2, respectively. For the 22 August event there is no prediction of UV emission (except at the end of the interval, 1004–1006 UT), but 2–3 kR is seen at T89 and T01 foot points. The maximum total electron energy flux measured by SC1 and SC4 is 2.0 mW/m^2 and 1.7 mW/m^2, respectively. For both these events the observed UV emissions increase (1634 UT and 0954 UT) almost at the same time as fast earthward flows (750 km/s and 1250 km/s) are observed (1636 UT and 0954 UT). For the 10 September event there are no predicted or observed UV emissions at the foot points. SC1, SC3 and SC4 measure the same maximum total electron energy flux, 0.4 mW/m^2.

[46] 4. The low maximum speed observed during the 10 September event is associated with very weak global auroral activity that might be characterized as a pseudo-breakup. The maximum *AE* value was only 38 nT.

2.3. Seven Events Without Imaging Data

[47] Finally, in Figure 7 we show the last seven events, where global imaging data and low altitude satellite data are not available. In column I the Cluster data are shown in the same format and same scales as in the previous figures. The flow speed V_x is high, 700–1400 km/s, for all the events except for 8 October 2001 (Figure 7b), ~640 km/s and 18 August 2002 (Figure 7d), ~470 km/s. The low maximum flow speed on 18 August 2002 is associated with very low *AE* index (maximum of 151 nT). *Åsnes et al.* [2008] studied the electron distribution observed by Cluster during this event, and because of the presence of significant fluxes of trapped electrons they concluded that this was probably a closed field line reconnection event.

[48] In columns II and III we show the predicted UV and X-ray emissions that would be observed in the ionosphere if the electrons leaving the reconnection region are not accelerated by any other mechanisms between the reconnection region and the ionosphere. In column IV the total electron energy flux are shown. Auroral predictions and energy flux for the different spacecraft are shown in black (SC1), green (SC3) and blue (SC4).

[49] As can be clearly seen, none of these events would produce any X rays that would have been observable in the ionosphere. For the UV emissions, the picture is somewhat different, with two events indicating no UV emissions (C-II and G-II) and 5 other with 1–1.5 kR (500–1000 counts), which cannot be considered as intense auroral activity. The maximum energy flux only reach 3.0 mW/m^2 for two of the events (B-IV and E-IV).

3. Discussion and Summary

3.1. Auroral Precipitation and Reconnection

[50] The main focus of this study is to answer the following question: Are electrons sufficiently accelerated in the reconnection region to produce observable auroral emissions in the conjugate ionosphere?

[51] We will first discuss the predicted X-ray emissions. As high energy electrons with hundreds of keVs have been observed [*Øieroset et al.*, 2002; *Åsnes et al.*, 2008] and predicted [*Pritchett*, 2006] one would expect that there should be X-ray emissions in ionosphere from these energetic electrons. While UV aurora is typically produced by 1–20 keV electrons, the production of X rays increases with electron energy. Of all the thirteen events, the combined PEACE and RAPID spectra only predict X-ray emissions for one event (17 August 2001). Although the predicted X rays are above the noise level for this event, the fluxes are very low and would be similar to what is seen at Cluster foot point (within the red circle) in Figure 5i and 5n. The one event reported by *Borg et al.* [2007] (Figure 5) is the only one where an intense X-ray spot has been seen simultaneously with the reconnection event in the tail. However, no X rays were predicted for this event and the DMSP spectra leaves no doubt that the electrons were accelerated by a potential drop. The electrons were accelerated somewhere outside the reconnection region.

[52] We have six events where predicted and observed UV emissions can be compared. For none of these events, except for 17 August 2001, which we will discuss below, did the PEACE/RAPID spectra predict UV emissions significantly above the noise level. The observed UV emissions in a ±1.5° longitudinal and ±0.5° latitudinal area around the T01 and T89 foot point of Cluster were generally much higher, i.e., ~2 kR, and even 6 kR for one event. For one event, 10 September 2001, no UV emissions were observed.

[53] For the seven events without imaging data the predicted UV emissions are just around the noise level for two of the events (Figures 7c-II and 7g-II) and weak for four other events (~800 R). Only one (B-II) of these events do the Cluster electron measurements predict significant UV aurora near the open-closed boundary.

[54] In Table 1 the maximum values of the 1-min average electron energy flux sampled in the outflow region are listed in the same sequence as we have presented each event in

this article. As UV emissions is roughly proportional to total electron energy flux, these values are consistent the maximum predicted UV emissions for each event. The values are overall small, except for the 17 August 2001 event. This is the event when the predicted UV emissions are in the same range as observed and the maximum energy flux reaches 8–11 mW/m^2. This may be related to the total field strength in the lobe that decreases from 60 nT to 40 nT from 1634 UT to 1640 UT, but stays constant after that (obtained by assuming pressure balance, but not shown). This change in the lobe field strength is a factor of 2 larger than during the three events where electron energy flux in the outflow region is only 2.6–2.7 mW/m^2 (1 October 2001, 8 October 2001 and 21 August 2002). This may imply that more magnetic energy was dissipated during the 17 August 2001 event.

[55] To summarize, we do not predict any measurable X rays for twelve of the events and for seven events the predicted UV emissions are zero or much lower than observed. Our results do not exclude the existence of acceleration mechanisms in the reconnection region that can produce electrons up to hundreds of keV [*Øieroset et al.*, 2002; *Åsnes et al.*, 2008] but they strongly indicate that the energy or the number fluxes of these electrons are too low to produce any auroral X-ray emissions. Although *Åsnes et al.* [2008] found energetic electrons in the 18 August 2002 event, the predicted X rays are zero. Our findings points to the conclusion that the total energization in the NENL reconnection region is marginal, in agreement with the calculation by *Yoon and Lui* [2006].

3.2. What are the Acceleration Mechanisms?

[56] If the acceleration in the reconnection region is marginal, what can then be the acceleration mechanisms responsible for the auroral intensities observed in the ionosphere? From the three events with low altitude satellite and global imaging data, we find electron distributions accelerated by potential drop or Alfvén waves near the open-closed boundary. However, DMSP and Cluster were not on conjugate field lines. During the one event where DMSP and Cluster were on conjugate field lines, i.e., on 2 October 2002, did we see plasma sheet electrons near the open-closed boundary and a strong potential drop equatorward of this. In addition to this we have two events without low-altitude satellite data indicating that the BBFs are causing the auroral emissions. The indication is that the discrepancy between observed and predicted emissions are seen coincidentally with the earthward flows on 17 August 2001 and 22 August 2001 (Figures 6H and 6i). Although this points to BBF being the acceleration mechanism we rather conclude that we are not able to answer the question about acceleration mechanism. We can only say that there has to be additional acceleration mechanism between the reconnection region and the ionosphere.

3.3. Substorm Relation

[57] The one event reported by *Borg et al.* [2007] is the only one where reconnection and auroral intensification were observed simultaneously. From four other events with global auroral imaging we can determine that substorm onset occurred 2–14 min before Cluster were inside the reconnection region. For two of the events in Figures 6H and 6i and the two events shown in Figures 4b and 4f, and Figures 5b and 5g, earthward flows are observed at the same time as the observed UV emissions (or X rays) increase at Cluster foot point. This gives some confidence in having both Cluster foot points and open-closed boundaries correctly determined. More important, though, this also indicates that reconnection is seen when the active region producing the auroral bulge reaches Cluster. Consequently, reconnection might be an expanding process observed along the poleward boundary of the aurora. Although the reconnection events reported here occur after the optical substorm onset, we cannot rule out that strong reconnection might have occurred in the sector of the auroral substorm onset at the time of the onset or even before, and that the reconnection region then expanded slowly toward the Cluster location.

4. Conclusions

[58] On the basis of thirteen events of in situ Cluster observations from the reconnection region we have examined whether magnetotail reconnection can produce the auroral intensities observed at the ionospheric foot point of the reconnection event. Our main findings are.

[59] 1. The electron distribution from the reconnection region can generally not produce the auroral intensities observed in the ionosphere. Only PEACE/RAPID spectra from six out of thirteen events predict auroral UV emissions significantly above the noise level of an instrument like IMAGE WIC and one of them predict any X rays above the noise level of an instrument like Polar PIXIE. For the six events we have global UV observations the predicted counts are much lower than what is observed at the T01 or T89 foot point of Cluster. Our results strongly indicate that acceleration in the reconnection region is usually marginal.

[60] 2. Particle data from low altitude satellite for three of the events indicate that the electrons observed near the open-closed boundary were accelerated by potential drop or Alfvén waves. The discrepancy seen in two events between observed and predicted emissions coinciding with earthward flows points to BBFs and potential drop. Although we can conclude that additional acceleration mechanism is needed, we are not able to identify the mechanism.

[61] 3. Our global imaging data show that reconnection is observed when global activity that started 2–14 min earlier reaches Cluster. This indicates that reconnection is an expanding process observed along the poleward boundary of the aurora.

[62] **Acknowledgments.** This study was funded by the Norwegian Research Council under contracts 170844 and 177272. The authors thank the Cluster CIS (PI Iannis Dandouras), FGM (PI Elizabeth Lucek), PEACE (PI Andrew Fazakerley), and RAPID (Patrick Daly) teams for providing the Cluster data used in this study. We also acknowledge Stephen Mende for the use of the IMAGE FUV data and Michael Schultz for the PIXIE data. The DMSP particle detectors were designed by Dave Hardy of AFRL, and data were obtained from JHU/APL. We thank Dave Hardy, Fred Rich, and Patrick Newell for their use. We acknowledge the World Data Center for Geomagnetism (T. Kamei), Kyoto, Japan, for providing the AE index.

[63] Wolfgang Baumjohann thanks Victor Sergeev for his assistance in evaluating this paper.

References

Angelopoulos, V., W. Baumjohann, C. F. Kennel, F. V. Coroniti, M. G. Kivelson, R. Pellat, R. J. Walker, H. Lühr, and G. Paschmann (1992), Bursty bulk flows in the inner central plasma sheet, *J. Geophys. Res.*, *97*(A4), 4027–4039.

Åsnes, A., M. G. G. T. Taylor, A. L. Borg, B. Lavraud, R. W. H. Friedel, C. P. Escoubet, H. Laakso, P. Daly, and A. N. Fazakerley (2008), Multispacecraft observation of electron beam in reconnection region, *J. Geophys. Res.*, *113*, A07S30, doi:10.1029/2007JA012770.

Baker, D. N., T. I. Pulkkinen, V. Angelopoulos, W. Baumjohann, and R. L. McPherron (1996), Neutral line model of substorms: Past results and present view, *J. Geophys. Res.*, *101*(A6), 12,975–13,010.

Balogh, A., et al. (2001), The cluster magnetic field investigation: Overview of in-flight performance and initial results, *Ann. Geophys.*, *19*(10–12), 1207–1217.

Baumjohann, W., G. Paschmann, and H. Lühr (1990), Characteristics of high-speed ion flows in the plasma sheet, *J. Geophys. Res.*, *95*(A4), 3801–3809.

Blanchard, G. T., L. R. Lyons, O. de la Beaujardiére, R. A. Doe, and M. Mendillo (1996), Measurements of the magnetotail reconnection rate, *J. Geophys. Res.*, *101*(A7), 15,265–15,276.

Borg, A. L. (2006), A study of magnetic reconnection events observed by the cluster satellites in the Earth's magnetotail, Ph.D. thesis, Univ. of Oslo, Oslo, Norway.

Borg, A. L., et al. (2007), Simultaneous observations of magnetotail reconnection and bright X-ray aurora on 2 October 2002, *J. Geophys. Res.*, *112*, A06215, doi:10.1029/2006JA011913.

Chaston, C. C., J. W. Bonnell, C. W. Carlson, J. P. McFadden, R. E. Ergun, and R. J. Strangeway (2003), Properties of small-scale Alfvén waves and accelerated electrons from FAST, *J. Geophys. Res.*, *108*(A4), 8003, doi:10.1029/2002JA009420.

Chaston, C. C., C. W. Carlson, J. P. McFadden, R. E. Ergun, and R. J. Strangeway (2007), How important are dispersive Alfvén waves for auroral particle acceleration?, *Geophys. Res. Lett.*, *34*, L07101, doi:10.1029/2006GL029144.

Crooker, N. U. (1986), An evolution of anti-parallel merging, *Geophys. Res. Lett.*, *13*(10), 1063–1066.

de la Beaujardiére, O., L. R. Lyons, and E. Friis-Christensen (1991), Sondrestrom radar measurements of the reconnection electric field, *J. Geophys. Res.*, *96*(A8), 13,907–13,912.

Dungey, J. W. (1961), Interplanetary magnetic field and the auroral zones, *Phys. Rev. Lett.*, *6*, 47–48.

Evans, D. S. (1974), Precipitating electron fluxes formed by a magnetic field aligned potential differences, *J. Geophys. Res.*, *79*(19), 2853–2858.

Frey, H. U., S. B. Mende, T. J. Immel, J. C. Gérard, B. Hubert, J. Spann, G. R. Gladstone, D. V. Bisikalo, and V. I. Shematovich (2003), Summary of quantitative interpretation of IMAGE ultraviolet auroral data, *Space Sci. Rev.*, *109*, 255–283.

Fujimoto, M., T. Nagai, N. Yokokawa, Y. Yamade, T. Mukai, Y. Saito, and S. Kokobun (2001), Tailward electrons at the lobe-plasma sheet interface detected upon dipolarization, *J. Geophys. Res.*, *106*(A10), 21,255–21,262.

Hardy, D. A., L. K. Schmitt, M. S. Gussenhoven, F. J. Marshall, H. C. Yeh, T. L. Shumaker, A. Hube, and J. Pantazis (1984), Precipitating electron and ion detectors (SSJ/4) for the block 5D/flights 6–10 DMSP satellites: Calibration and data presentation, *Tech. Rep. AFGL–TR-84-0317*, Air Force Geophys. Lab., Hanscom Air Force Base, Mass.

Hubert, B., S. Milan, A. Grocott, C. Blockx, S. W. H. Cowley, and J. C. Gerard (2006), Dayside and nightside reconnection rates inferred from IMAGE FUV and Super Dual Auroral Radar Network data, *J. Geophys. Res.*, *111*, A03217, doi:10.1029/2005JA011140.

Imada, S., R. Nakamura, P. W. Daly, M. Hoshino, W. Baumjohann, W. S. Muhlbachler, A. Balogh, and H. T. Reme (2007), Energetic electron acceleration in the downstream reconnection outflow region, *J. Geophys. Res.*, *112*, A03202, doi:10.1029/2006JA011847.

Imhof, W. L., et al. (1995), The Polar Ionospheric X-ray Imaging Experiment (PIXIE), *Space Sci. Rev.*, *71*, 385–408.

Johnstone, A. D., et al. (1997), PEACE: A Plasma Electron and Current Experiment, *Space Sci. Rev.*, *79*, 351–398.

Kaymaz, Z., G. L. Siscoe, N. A. Tsyganenko, and R. P. Lepping (1994), Magnetotail views at 33 RE: IMP 8 magnetometer observations, *J. Geophys. Res.*, *99*(A5), 8705–8730.

Khrabrov, A. V., and B. U. Ö. Sonnerup (1998), Error estimates for minimum variance analysis, *J. Geophys. Res.*, *103*(A4), 6641–6651.

Lockwood, M. (1997), Identifying the open-closed field line boundary, in *Polar Cap Boundary Phenomena*, edited by J. Moen, A. Egeland, and M. Lockwood, pp. 73–90, Springer, in cooperation with NATO Scientific Affairs Division, Dordrecht, Netherlands.

Lyons, L., E. Zesta, Y. Xu, E. R. Sánchez, J. C. Samson, G. D. Reeves, J. M. Ruohoniemi, and J. B. Sigwarth (2002), Auroral poleward boundary intensifications and tail bursty flows: A manifestation of a large-scale UL Foscillation?, *J. Geophys. Res.*, *107*(A11), 1352, doi:10.1029/2002JA000242.

Mende, S. B., et al. (2000), Far ultraviolet imaging from the IMAGE spacecraft: 2. Wideband FUV imaging, *Space Sci. Rev.*, *91*, 271–285.

Milan, S. E., G. Provan, and B. Hubert (2007), Magnetic flux transport in the Dungey cycle: A survey of dayside and nightside reconnection rates, *J. Geophys. Res.*, *112*, A01209, doi:10.1029/2006JA011642.

Nagai, T. (2006), Location of magnetic reconnection in the magnetotail, *Space Sci. Rev.*, *122*, 39–54.

Nakamura, R., W. Baumjohann, M. Brittnacher, V. Sergeev, M. Kubyshkina, T. Mukai, and K. Liou (2001), Flow burst and auroral activations: Onset timing and foot point location, *J. Geophys. Res.*, *106*(A6), 10,777–10,789.

Ober, D. M., N. C. Maynard, W. J. Burke, W. K. Peterson, J. B. Sigwarth, L. A. Frank, J. D. Scudder, W. J. Hughes, and C. T. Russell (2001), Electrodynamics of the poleward auroral border observed by Polar during a substorm on April 22, 1998, *J. Geophys. Res.*, *106*(A4), 5927–5943.

Øieroset, M., R. P. Lin, T. D. Phan, D. E. Larson, and S. D. Bale (2002), Evidence for electron acceleration up to ∼300 keV in the magnetotail reconnection diffusion region of Earth's magnetotail, *Phys. Rev. Lett.*, *89*(19), 195001, doi:10.1103/PhysRevLett89.195001.

Østgaard, N., J. Stadsnes, J. Bjordal, R. R. Vondrak, S. A. Cummer, D. Chenette, M. Schulz, and J. Pronko (2000), Cause of the localized maximum of X-ray emission in the morning sector: A comparison with electron measurements, *J. Geophys. Res.*, *105*(A9), 20,869–20,885.

Østgaard, N., J. Stadsnes, J. Bjordal, G. A. Germany, G. K. Parks, R. R. Vondrak, S. A. Cummer, D. Chenette, and J. Pronko (2001), Auroral electron distributions derived from combined UV and X-ray emissions, *J. Geophys. Res.*, *106*(A11), 26,081–26,090.

Østgaard, N., J. Moen, S. B. Mende, H. U. Frey, T. J. Immel, P. Gallop, K. Oksavik, and M. Fujimoto (2005), Estimates of magnetotail reconnection rate based on IMAGE FUV and EISCAT measurements, *Ann. Geophys.*, *23*(1), 123–134.

Pritchett, P. L. (2006), Relativistic electron production during driven magnetic reconnection, *Geophys. Res. Lett.*, *33*, L12104, doi:10.1029/2005GL025267.

Reme, H., et al. (2001), First multispacecraft ion measurements in and near the Earth's magnetosphere with the identical Cluster Ion Spectrometry (CIS) experiment, *Ann. Geophys.*, *19*(10–12), 1303–1354.

Runov, A., et al. (2008), Observations of an active thin current sheet, *J. Geophys. Res.*, *113*, A07S27, doi:10.1029/2007JA012685.

Sergeev, V. A., et al. (2008), Study of near-Earth reconnection events with Cluster and Double Star, *J. Geophys. Res.*, *113*, A07S36, doi:10.1029/2007JA012902.

Shiokawa, K., W. Baumjohann, G. Haerendel, and H. Fukunishi (2000), High- and low-altitude observations of adiabatic parameters associated with auroral electron precipitation, *J. Geophys. Res.*, *105*(A2), 2541–2550.

Snekvik, K., R. Nakamura, N. Østgaard, S. Haaland, and A. Retino (2008), The Hall current system revealed as a statistical significant pattern during fast flows, *Ann. Geophys.*, *26*(11), 3429–3437.

Sonnerup, B. U. O. (1979), Magnetic field reconnection, in *Solar System Plasma Physics*, edited by C. F. Kennel, L. J. Lanzerroti, and E. N. Parker, pp. 45–108, Elsevier, Amsterdam.

Treumann, R. A., C. H. Jaroschek, R. Nakamura, A. Runov, and M. Scholera (2006), The role of the Hall effect in collisionless magnetic reconnection, *Adv. Space Res.*, *38*, 101–111, doi:10.1016j.asr.2004.11.045.

Tsyganenko, N. A. (1989), A magnetospheric magnetic field model with a warped tail current sheet, *Planet. Space Sci.*, *37*(1), 5–20.

Tsyganenko, N. A. (1995), Modelling the Earth's magnetospheric magnetic field confined within a realistic magnetopause, *J. Geophys. Res.*, *100*(A4), 5599–5612.

Tsyganenko, N. A. (2002), A model of the near magnetosphere with a dawn-dusk asymmetry: 2. Parametrization and fitting to observations, *J. Geophys. Res.*, *107*(A8), 1179, doi:10.1029/2001JA000220.

Ueno, G., S. Othani, T. Mukai, Y. Saito, and H. Hayakawa (2003), Hall current system around the magnetic neutral line in the magnetotail: Statistical study, *J. Geophys. Res.*, *108*(A9), 1347, doi:10.1029/2002JA009733.

Vasyliunas, V. M. (1984), The last words, in *Magnetic Reconnection in Space and Laboratory Plasmas*, *Geophys. Monogr. Ser.*, vol. 30, edited by E. W. Hones Jr., pp. 385–386, AGU, Washington, D. C.

Wilken, B., et al. (2001), First results from the RAPID imaging energetic particle spectrometer on board Cluster, *Ann. Geophys.*, *19*(10–12), 1355–1366.

Wygant, J. R., et al. (2000), Polar spacecraft based comparisons of intense electric fields and Poynting flux near and within the plasma sheet-tail lobe boundary to UVI images: An energy source for the aurora, *J. Geophys. Res.*, *102*(A8), 18,675–18,692.

Yoon, P. H., and A. T. Y. Lui (2006), Energy conversion during magnetic reconnection for magnetotail-like equilibria, *Phys. Plasmas*, *13*, 102303.

A. Åsnes, SRE-OSC, ESTEC, Keplerlaan 1, 220AG Noordwijk, Netherlands.

A. L. Borg, Norwegian Defence Research Establishment, Box 25, N-2027 Kjeller, Norway.

S. E. Haaland, N. Østgaard, and K. Snekvik, Department of Physics and Technology, University of Bergen, Room 449, Allegt. 55, N-0007 Bergen, Norway. (nikolai.ostgaard@ift.uib.no)

M. Øieroset and T. Phan, Space Sciences Laboratory, University of California, 7 Gauss Way, Berkeley, CA 94720-7450, USA.

A. Pedersen, Department of Physics, University of Oslo, Box 1048-Blindern, N-0316 Oslo, Norway.